7th International Conference on Silicon Photovoltaics, SiliconPV 2017

Comparison of drone-based IR-imaging with module resolved monitoring power data

Janine Teubner[a,*], Ingmar Kruse[b], Hans Scheuerpflug[a], Claudia Buerhop-Lutz[a], Jens Hauch[a], Christian Camus[a], Christoph J. Brabec[c,a]

[a]*Bavarian Center for Applied Energy Research, Immerwahrstraße 2, Erlangen 91058, Germany*
[b]*SunSniffer GmbH & Co. KG, Ludwig-Feuerbach-Straße 69, Nuremberg 90489, Germany*
[c]*Institute Materials for Electronics and Energy Technology, Martenstraße 7, Erlangen 91058, Germany*

Abstract

Two testing methods for photovoltaic (PV) plants, an infrared (IR)-measurement aerial system and a monitoring system on module level, are compared with respect to their capabilities for identifying irregularities of PV panels in a PV plant.

For the first method, a hypothesis is tested that infrared temperature and module power can be correlated with an empirical linear correlation using the raw measurement data of the second method. A workaround is proposed how to quantify power losses for unknown PV plants showing at the same time how power losses depend on ambient conditions. Also, the data is used to improve results from the IR-measurements. The second method is explained to compare the two methods. It is shown that each method offers different advantages, helping to properly assess and schedule O&M measures.

© 2017 The Authors. Published by Elsevier Ltd.
Peer review by the scientific conference committee of SiliconPV 2017 under responsibility of PSE AG.

Keywords: IR thermography; UAV; inspection; silicon photovoltaics; reliability; power loss correlation

1. Introduction

In the past years, reliability and maintenance of solar power plants have seen growing interest. The importance of quality inspection lays in the impact which defective photovoltaic (PV) modules can have on power output as well

* Corresponding author. Tel.: +49 9131 9398-175; fax: +49 9131 9398-199.
 E-mail address: janine.teubner@zae-bayern.de

as on the safety of all modules in the same string. Drone-mounted infrared (IR) measurement systems (like *aIR-PV-check*) present already a well-known, fast and easy method to detect modules with irregular temperature patterns, a reliable indicator of defects (see [1], [2] for further explanations). But the nature and severity of the so-found suspicious sites are not perfectly clear up to now, although a lot of research has already been conducted in that direction [3]. If it was possible to quantify all modules' power losses, maintenance of solar power plants could be optimized even further. The module-resolved SunSniffer® measurement system is a new promising method which continuously measures the voltage and junction box temperature of every single module.

This study compares the two testing methods with respect to their capabilities for identifying irregularities of PV panels in a PV plant and combines their relevant findings. For the SunSniffer system, the measurement data is validated by comparison to whether or not thermal irregularities are found. For aIR-PV-check, an empirical approach is followed for correlating the module temperatures measured via IR to their respective electrical power generation losses. According to the law of energy conservation, the mean module temperature should be the higher the lower the power output is.

2. Method and experimental procedure

2.1. Explanation of the SunSniffer system

The SunSniffer system consists of the measuring units attached to each module which measure each module's voltage and junction box temperature with a high temporal resolution as well as the evaluation engine and an online portal which makes the measurements accessible [4], [5]. The main aim of the SunSniffer engine is to define the *health status* of modules thus identifying weak modules and defects like PID or LID while distinguishing these from shadowing in order to be able to eventually suggest module replacements. As SunSniffer directly measures electrical data, it is known which defects really are power-relevant. Thus, the measurement data act as a reference for the aIR-PV-check data. Analysis of the data quality shows that 500 out of 510 modules yielded usable data during the measurement period. Generally, modules may have a different instantaneous power reduction depending on the ambient conditions as can be seen in Fig. 1 which shows the continuously measured electrical data from SunSniffer: The module voltage changes depending on the ambient conditions. Thus, also the power loss changes.
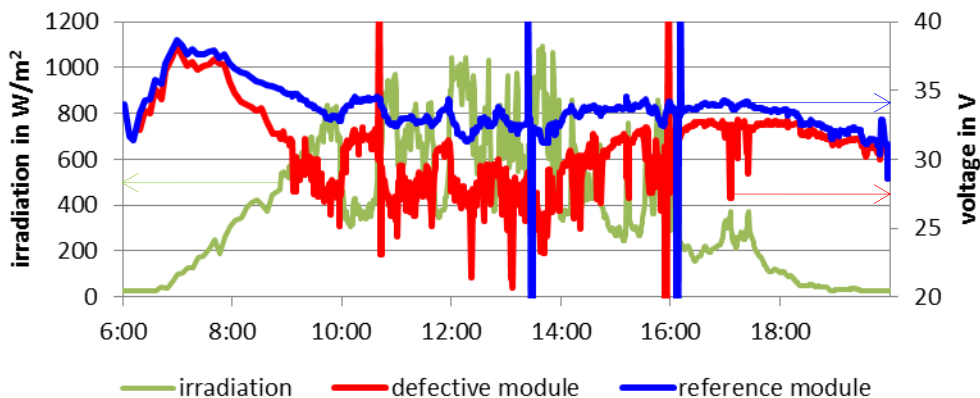

Fig. 1. The measured module voltages of a power-reduced module and its reference as well as the irradiance on 04.08.2016

2.2. Processing data for correlation of module power and temperature with aIR-PV-check

For assessing module powers by their temperatures by aIR-PV-check, the total energy balance of a PV module is evaluated which allows calculating the module power from the mean module temperature and the ambient conditions as well as their distribution. But especially the wind speed distribution governing the heat losses is

complex to calculate (see [6]). Thus, an empirical correlation for a given set of environmental parameters may prove easier in practice. Additionally, in order to minimize IR measurement uncertainties, the module temperature is pre-processed by calculating the module temperature difference using the mean module temperatures of a power-reduced module $\bar{T}_D$ and a suitable non-defective reference module of the same string $\bar{T}_{ND}$ using aIR-PV-check:

$$\Delta T = \bar{T}_D - \bar{T}_{ND} \tag{1}$$

The index *D* indicates a *defective*, *ND* a *non-defective* module. The mean module temperatures are the IR temperatures of one module averaged over the whole module area. The module power varies depending on the severity of the defect. Hence, it is normalized by using a reference module of the same string; so that the relative module power P_{rel} can be obtained by dividing the corresponding module voltages (see Eq. (2)).

In order to attain reliable data, a roof-mounted PV plant equipped with the module-resolved SunSniffer® system was inspected by aIR-PV-check. The plant is located in Cadolzburg, Middle Franconia (plant C), with a total power of 100 kWp and 510 modules. It was measured on 04.08.2016 from 12:00-12:11 at an irradiation of 950 W/m^2 and an ambient temperature of 26°C. As shown in Fig. 1, the module voltages change and since aIR-PV-check is an instantaneous measurement method, the module voltages used are averaged over the IR measurement period: During the aIR-PV-check period, relatively constant ambient conditions were ensured. The corresponding measurement data taken from the SunSniffer system was averaged over the same period to make it comparable to aIR-PV-check, described with $\Delta t_{IR} = t_{e,IR} - t_{b,IR}$ with $t_{b,IR}$ being the time beginning and $t_{e,IR}$ being the end of the IR measurement:

$$P_{rel}(E(t_{IR}), T_U(t_{IR}), v(t_{IR})) = \frac{P_D}{P_{ND}}\bigg|_{t_{IR}} \approx \frac{\bar{U}_D}{\bar{U}_{ND}} = \frac{\frac{\sum_{t=t_{b,IR}}^{t=t_{e,IR}} U_D(t)}{n_D}}{\frac{\sum_{t=t_{b,IR}}^{t=t_{e,IR}} U_{ND}(t)}{n_{ND}}} = \frac{U_D}{U_{ND}}\bigg|_{\Delta t_{IR}} \tag{2}$$

U_D is the voltage of the defective module, n_D the number of measuring points of U_D during Δt_{IR}, U_{ND} is the voltage of the non-defective reference module while n_{ND} indicates the number of measuring points of U_{ND} during Δt_{IR}. P is the module's power. To facilitate the manual data processing, the pre-analyzed power loss data supplied by the SunSniffer software was used to filter the modules in advance. To determine a sensitive power loss limit, some strings' module powers were analyzed which appeared to be perfectly fine. One string differed by 4% in power losses, another one showed a variation of 3%. Also, the uncertainty of the modules' power amounts to 3% as given by the manufacturer. Thus, a sensitive power loss threshold of 3% is considered sufficiently high for filtering the naturally occurring power fluctuations whilst being low enough to be a sensitive power loss threshold.

The relative power for each pre-filtered module was calculated according to equation (2) and correlated to the module temperature differences obtained from the IR images according to equation (1). Fig. 2 (left) depicts the IR image taken of one module exhibiting an inhomogeneous temperature pattern. A superimposed pattern due to convection can clearly be seen as the lower row of modules is noticeably colder, so the reference module has to be chosen with care. It should be in a similar convective environment, thus, a module in the same row next to the defective module was chosen in this example. In Fig. 2 (right), the module voltage is found to be lower than its reference equaling a mean relative power loss of 13% averaged over the aIR-measurement time period. The mean module temperature amounts to 51.9 °C while the maximum module temperature is 63.2 °C. The mean reference module temperature is 50.9 °C resulting in a mean module temperature difference of 1 K. As can be seen, even a seemingly minor temperature difference of the mean module temperatures of 1 K can be related to a non-negligible power loss of over 10%.
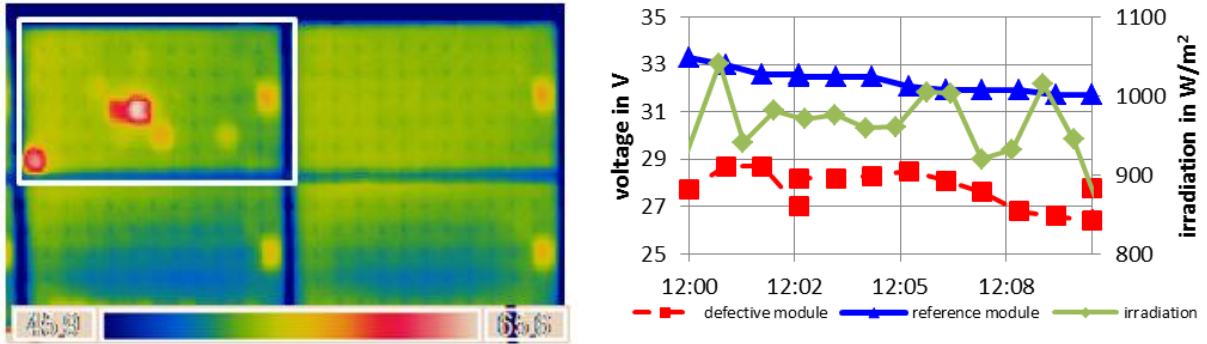
Fig. 2. Left: The IR image shows the module from Fig. 1 which exhibits temperature irregularities (white rectangle). Right: Voltage over time for the same module and the reference module next to it during the aIR-measurement interval from the SunSniffer system.

Then, in order to gain a correlation for a second set of ambient parameters, a plant on an industrial building in Nuremberg (plant N) was measured on 01.09.2016 from 14:00-16:00 with an irradiation of 440 W/m^2 and an ambient temperature of 30°C. It consists of several roofs with 4552 solar modules amounting to 1092 kWp. The latter is not fully equipped with SunSniffer and allows no allocation of modules. Therefore, the results from plant C are applied and modified to assess the modules found via aIR-PV-check in plant N.

3. Results

3.1. Empirical correlation of module power and temperature

In Fig. 3 (left), the mean relative power is plotted over the module temperature differences using the modules found via aIR-PV-check. The mean temperature of one substring in open circuit was measured in order to approximate the temperature of a module operating in open circuit (meaning that the entire amount of energy from absorption is dissipated as heat). The mean temperature of one open-circuited substring is considered a good approximation of a whole module in open circuit since it exhibits a very homogenous temperature distribution. The result was added to
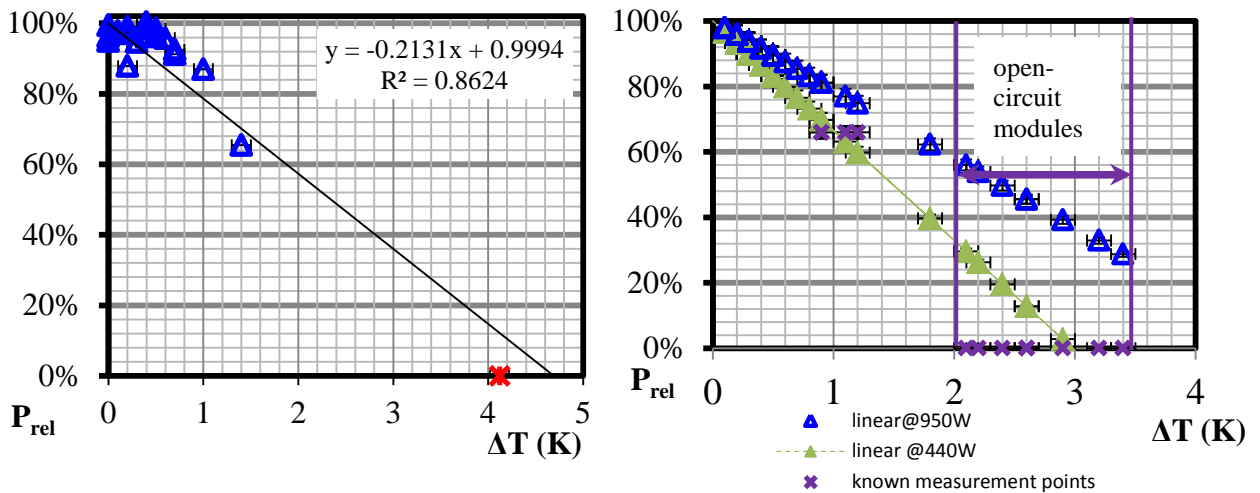

Fig. 3. Left: Correlation of the relative module power with the module temperature differences for plant C (pre-refinement) with linear fit and error bars indicating the repeatability measurement uncertainty of the IR camera. The constructed data point for an open-circuit module is marked with a red star. Right: Application of the correlation found with plant C (linear@950W) to plant N (linear@440W)

the chart as a further theoretical data point and visually set apart. The data is fitted to a linear function. It can be seen that the lower the relative power and the higher the relative power losses, the higher are the temperature differences. Some scattering is present (R^2=0.8604). Power losses deviate with up to 0.12 when considering, and with up to 0.09 when neglecting the constructed open circuit point. Next, the correlation deduced is applied to plant N. For plant N, only the module temperatures are known. In Fig. 4 (right), the relative module power is plotted over the module temperature differences which were calculated using the correlation of plant C. Data points with known relative power are added for validation which are given by modules in open circuit (relative power equals zero) or modules with a disconnected substring (relative power is reduced by one third). Modules in open-circuit or with missing substrings are easily identified by aIR-PV-check, see [1], [2]. As can be seen in Fig. 4 on the right, the linear correlation deduced at 950 W/m^2 (from plant C) does not yield a good approximation. This indicates that the correlation depends on the irradiation as plant N was measured at a far lower irradiation. In order to adapt the correlation to 440 W/m^2 (plant N), the data points with known relative power are used to modify the linear correlation. They are marked with violet crosses. Then, the curve's slope was increased until the linear function gives a good approximation of the known data points. This confirms that the lower the relative power is, the higher are the temperature differences. The horizontal error bars give the repeatability measurement inaccuracy of the IR camera, the vertical ones the error to be expected by the power variations of the reference modules (see 2.2).

3.2. Comparison of SunSniffer and aIR-PV-check

The SunSniffer measurement data is invaluable for refining aIR-PV-check assessment criteria quantitatively as it originally constitutes a mainly qualitative method depending on personal experience. Fig. 4 gives an example for a module that was previously (pre-refinement) not assessed as thermally suspicious (marked with a white frame). Consulting the SunSniffer measurement data, it exhibits a power loss of 2.9%, being close to the manufacturer's tolerance limit. Upon closer inspection, it indeed shows an irregular temperature pattern at its lower edge. All suspicious modules detectable through the SunSniffer measurement system that were initially not detected by aIR-PV-check were compared with other modules in their surroundings with respect to if they distinguish themselves by irregular or stronger irregular temperature patterns in comparison (called refinement).
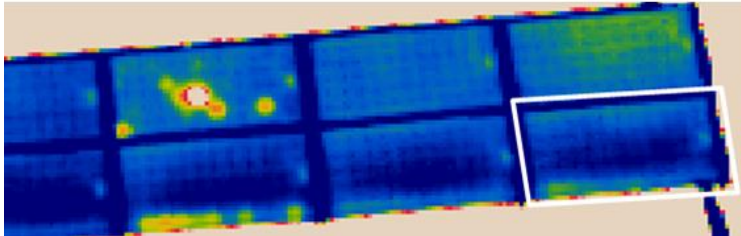

Fig. 4. An example of an *aIR-PV-check* refinement: The marked module exhibits an irregular temperature pattern and 2.9% power loss when consulting the SunSniffer measurement data.

Table 1 presents the number of modules identified by aIR-PV-check pre- and post-refinement in comparison to the SunSniffer measurement data for different power loss ranges. It can be seen that with aIR-PV-check, fewer modules are detectable in the lower power loss ranges prior to refinement than based on the SunSniffer measurement data. Through refinement, most modules are qualitatively detectable which are above the power loss threshold of 3% as defined in 2.2. For higher power loss ranges larger than 5%, no module is missed even before refinement.

It follows that a high number of modules exhibits calculated power losses lower than 3%. Of these, only a fraction was also suspicious in aIR-PV-check. One module supposedly exhibiting power loss in the range 3-5% has no detectable irregular temperature pattern at all; the module could be lower in power due to manufacturing or it degraded homogenously. Also, it may be labeled falsely in the module allocation system. Furthermore, the power distribution for the correlated power data is added in Table 1. It can be seen that the distribution spreads more widely as the number of modules with a calculated relative power loss below zero and above 10% increase which

mostly are misinterpreted modules from the low power range. Calculating the standard deviation from the measurement data with factor two according to 95% confidence interval leads to a "measurement uncertainty" of 8.3%. In Table 2, the properties of both methods are compared.

Table 1. Distribution of detected modules using the SunSniffer measurement data, aIR-PV-check before and after refinement and the correlation data of aIR-PV-check

Calculated instantaneous relative power loss eq. (2)	# modules (SunSniffer measurement data)	# modules (aIR pre-refined)	# modules (aIR refined)	# modules (aIR correlation data)
<0%	21	2	2	6
0%-3%	34	12	29	4
3%-5%	11	5	10	6
5%-10%	5	5	5	4
>10%	3	3	3	7
minimum relative power loss	0.3%	-1.1%	-1.1%	-10.5%
maximum relative power loss	34.6%	34.6%	34.6%	29.3%

Table 2. Comparison of features between the SunSniffer system and aIR-PV-check

Comparison of features	SunSniffer	aIR-PV-check
time scale	long-term	instantaneous
defect resolution	module level	locally resolved within module
defect classification	some defects like diode failures	most defects through defect pattern
PV plants applicable	installed	flexible
measurement uncertainty	1.0%	8.3%

4. Discussion

Considering the correlation in 3.1, a relationship can be seen between lower relative module power and higher module temperature difference which meets the initial expectations. Yet, the measurement uncertainty of 8% is high compared to SunSniffer which is due to convection especially when the reference module is not in the same convective environment. Also, in the lower temperature regime, some non-linear influences are present which is plausible considering that radiation depends on the fourth order of temperature so the linear fit does maybe not present an accurate mathematical description. In [7], a logistic fit was chosen without explanation. The deviation of the constructed open-circuit point is also likely due to convection because a substring on the edge was used which is usually cooler than the middle substring. It follows that a substring may be used as an approximation for an open-circuit module but some deviation can be expected (<1 K). The wide spreading of the open-circuit-modules again accounts for differing convective environments in Fig. 3 (right). A superimposed pattern due to convection was existent similar to Fig. 2 (left) and Fig. 6. Due to that, often an appropriate reference module cannot be found. It follows that convection plays a major role in this analysis and the choice of a suitable reference module is crucial. Considering the refinement undertaken by using the measurement data, it is clear that qualitatively, almost every power-reduced module exhibits thermal irregularities making it detectable. The power loss limit of 3% is sensible as misinterpretations below that are probable. Generally, the PV plant investigated is in good condition as only a few

defective modules are present. With more defective modules, a larger range of the correlation could have been assessed. Known measurement points can be used to approximate a correlation and it becomes clear that the presented power losses are only valid for the given ambient conditions so further analysis will focus on elucidating the dependency on the ambient conditions. When comparing SunSniffer measurement data and aIR-PV-check, both methods confirm each other's findings by identifying the same power-reduced modules especially for higher power losses whilst SunSniffer has a far lower measurement uncertainty than aIR-PV-check. Because of that, the assessment of power losses should be combined with the IR defect pattern as can be seen in Table 1 where the number of qualitatively detected modules is high. The SunSniffer system on the other hand measures and monitors module powers thus always knowing power losses while aIR-PV-check can be applied on every plant as it is an instantaneous method and can also easily identify defect causes.

5. Conclusion

SunSniffer and aIR-PV-check are different measurement techniques which were compared in this study leading to some important insights for the benefit of both methods. So it became clear that irregular temperature patterns correspond well with significant power losses and can be correlated quantitatively. A clear relationship could be seen between lower relative module power and higher module temperature difference allowing quantifying power losses of a module with an uncertainty of fewer than 10%. Yet, the correlation may not be linear. The application of the correlation to plant N was possible, but for a complete evaluation of the prediction, the results should be compared with lab measurements. Further experiments should be conducted preferably with PV plants in the field in order to compare and refine the results. The aIR-PV-check assessment criteria were found to underestimate power losses below 5% mainly due to the production fluctuations. Altogether, it becomes clear that for higher power losses, SunSniffer and aIR-PV-check affirm each other's findings, identifying the same power-reduced modules. In comparison to aIR-PV-check, SunSniffer directly measures electrical data so it is known which defects really are power-relevant. The root cause remains unknown, though. On the other hand, aIR clearly reveals any thermal inhomogeneity of modules and may indicate defect causes but will not necessarily know any power losses, so the severity of the loss may not be assessed in any case. Both methods benefit from each other since SunSniffer helped deduce more specific *aIR-PV-check* assessment criteria while aIR offers the opportunity to identify typical failure modes of modules, which may be used in the future to train SunSniffer in order to identify these modes based on the temporal changes of the data gathered from these modules.

References

[1] Cl. Buerhop, D.Schlegel, M.Niess, C.Vodermayer, R.Weißmann, C.J.Brabec, "Reliability of IR-imaging of PV-plants under operating conditions", Solar Energy Materials & Solar Cells 107, 154–164 (2012)
[2] Cl. Buerhop, R. Weißmann, H. Scheuerpflug, R. Auer, C. Brabec, "Quality Control of PV-Modules in the Field Using a Remote-Controlled Drone with an Infrared Camera", 27th EUPVSEC (2012)
[3] R. Moretón, E. Lorenzo and L. Narvarte, "Experimental observations on hot-spots and derived acceptance/rejection criteria", Solar Energy 118, 28-40 (2015)
[4] G. Behrens, A. Domnik, S. Hempelmann, J. Weicht, F. Hamelmann, S. Yilmaz, I. Kruse: „ Machine learning methods for partial shading detection in monitoring data on PV-systems ", 29th European Photovoltaic Solar Energy Conference and Exhibition (2014)
[5] G. Behrens, F. Hamelmann, S. Yilmaz, I. Kruse, J. Weicht, L. Niemann: „Universal location based data sets for monitoring and scientific data analysis of PV-systems", 28th European Photovoltaic Solar Energy Conference and Exhibition (2013)
[6] D. Torres Lobera, S. Valkealahti: "Dynamic thermal model of solar PV systems under varying climatic conditions", Solar Energy 93 (2013) 183–194
[7] T. Kaden, K. Lammers and H. J. Möller, "Power loss prognosis from thermographic images of PID affected silicon solar modules", Solar Energy Materials & Solar Cells 142, 24-28 (2015)